Synthesis, electrochemistry, structure, and magnetic susceptibility of 5-*tert*-butyl-1,3-bis-(1,2,3,5-dithiadiazolyl)benzene. Structural effect of the bulky substituent[1]

Richard A. Beekman, René T. Boeré, Klaus H. Moock, and Masood Parvez

Abstract: The crystal structure of the title compound was determined at 250 K in space group $I\bar{4}2m$, $a = 20.661(5)$ Å, $c = 6.764(7)$ Å, $Z = 8$. The individual dithiadiazole rings form two sets of contrarotatory 4-member pinwheels clustered around a 4-fold rotation–inversion axis located halfway along the unit cell edges, describing an infinite channel lined with sulfur atoms but in which there are short intra-stack contacts through only one S atom of each CN_2S_2 group. The double-layer stacking occurs in order to accommodate the bulk of the ^{t}Bu group, and the spacing between layers is very regular, with short and long S···S contacts of 3.48(2) and 3.61(2) Å and considerable thermal motion in the *c* direction. The title compound and its SbF_6^- salt are oxidized at +0.81 V (in CH_2Cl_2) and at +0.61 V (in CH_3CN), while a reduction process is observed only in CH_2Cl_2 at –0.73 V vs. SCE. Magnetic susceptibility data between 5 and 400 K demonstrate at very low temperature that the sample follows the Curie–Weiss law, $\theta = 0$ K, and $\chi_0 = -156$ ppm emu mol^{-1}. The free-spin concentration at $T = 0$ K is ≈1.3%, due to paramagnetic defects in an essentially diamagnetic structure. The diamagnetism starts to lift above 210 K; above 260 K, a strong antiferromagnetic exchange is operative. These results are consistent with the lifting of the Peierls distortion in this structure, starting above ≈200 K. The crystal structure of the parent diamidine 5-*tert*-butyl-1,3-$[(Me_3Si)_2NCNSiMe_3]_2C_6H_3$ was determined in $C2/c$ with $a = 10.0788(3)$, $b = 21.328(5)$, $c = 20.876(5)$ Å, $\beta = 99.41(2)°$, $Z = 4$. The two amidine functional groups are equivalent by crystal symmetry.

Key words: dithiadiazole, diradical, magnetic susceptibility, crystal structure, bulky substituent.

Résumé : On a déterminé la structure cristalline du composé mentionné dans le titre à 250 K; il cristallise dans le groupe d'espace $I\bar{4}2m$ avec $a = 20{,}661(5)$ Å, $c = 6{,}754(7)$ Å et $Z = 8$. Les noyaux dithiadiazoles individuels forment deux ensembles à sens contraire, en forme de moulinet à quatre membres, regroupés autour d'un axe de rotation–inversion quaternaire situé à mi-chemin le long des arêtes du motif élémentaire et décrivant un canal infini bordé d'atomes de soufre; on n'y observe toutefois qu'un seul point de contact court entre les empilements et il se produit entre un atome de soufre de chaque groupe CN_2S_2. L'empilement à deux couches se produit de façon à accommoder l'encombrement du groupe *tert*-butyle et la distance entre les couches est très régulière alors que les distances S···S courtes et longues sont respectivement de 3,48(2) et 3,61(2) Å et qu'on observe beaucoup de mouvement thermique dans la direction *c*. Le composé mentionné dans le titre et son sel de SbF_6^- sont oxydés à +0,81 V (dans le CH_2Cl_2) et à +0,61 V (dans le CH_3CN) alors que l'on n'observe le processus de réduction que dans le CH_2Cl_2, à –0,73 V vs. SCE. Les données de susceptibilité magnétique entre 5 et 400 K démontrent que, à température très basse, l'échantillon obéit à la loi de Curie–Weiss, $\theta = 0$ K et $\chi_0 = -156$ ppm emu mol^{-1}. La concentration libre de spin à $T = 0$ K est égale à 1,3% à cause de défauts paramagnétiques dans une structure essentiellement diamagnétique. Le diamagnétisme commence à s'éliminer et, au-dessus de 260 K, un important échange antiferromagnétique est en action. Ces résultats sont en accord avec l'élimination progressive de la distorsion de Peierls dans cette structure à partir d'environ 200 K. On a déterminé la structure cristalline de la diamine parent, 5-*tert*-butyl-1,3-$[(Me_3Si)_2NCNSiMe_3]_2C_6H_3$, qui cristallise dans le groupe d'espace $C2/c$, avec $a = 10{,}0788(3)$, $b = 21{,}328(5)$ et $c = 20{,}876(5)$ Å, $\beta = 99{,}41(2)°$ et $Z = 4$. Les deux groupes fonctionnels amidines sont équivalents par symétrie cristalline.

Mots clés : dithiadiazole, diradical, susceptibilité magnétique, structure cristalline, substituant encombrant.

[Traduit par la rédaction]

Received July 8, 1997.

R.A. Beekman and R.T. Boeré.[2] Department of Chemistry, University of Lethbridge, Lethbridge, AB T1K 3M4, Canada.

K.H. Moock. Research School of Chemistry, Australian National University, Canberra, ACT 0200, Australia.

M. Parvez. Department of Chemistry, University of Calgary, Calgary, AB T2N 1N4, Canada.

[1] Presented in part at the 80th Canadian Society for Chemistry Conference, Windsor, Ontario, July 1–4, 1997.

[2] Author to whom correspondence may be addressed. Telephone: (403) 329-2045. Fax: (403) 329-2057. E-mail: boere@uleth.ca

Introduction

1,2,3,5-Dithia- and diselena-diazoles, **1**, have been extensively investigated as potential single-component molecular conductors (1). Early examples formed isolated dimer pairs, as in the first structurally characterized compound, 4-phenyl-1,2,3,5-dithiadiazole (2). Molecular engineering has focused on obtaining solids in which the heterocycles are stacked into infinite arrays in the solid, yet in all cases where stacking is observed for neutral systems, the *spacing* of the layers alternates between short and long separation. This has been interpreted as the result of a Peierls distortion (3). There is evidence from magnetic measurements that this distortion may be overcome at a higher temperature for the neutral derivatives, and it

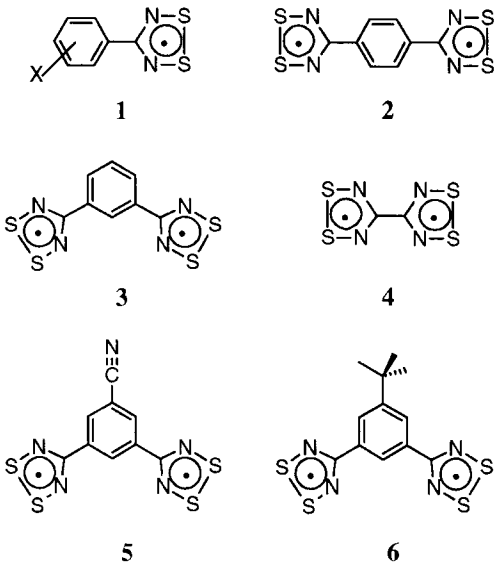

is overcome in some systems by partial oxidation (4). Up till now the main strategies used to overcome this inherent tendency to distortion have been (*i*) to minimize the bulk of the R-group, e.g., **1**, but with the aromatic ring replaced only by an H atom (5), or by increasing the nuclearity of the dithiadiazole centres to include bi- and tri-functional species such as **2** (6), **3** (7), or **4** (8); and (*ii*) through the inclusion of ancillary donor sites (e.g., nitrile on (9–11) or nitrogen *within* (12) the aryl backbone), as in **5** (9). Recently, the latter strategy applied to 4-$NCC_6F_4CN_2S_2$ resulted, due to strong interaction with the nitrile groups, in a sheet structure that, while evenly spaced, has no vertical stacks at all; consistently this material behaves as a bulk paramagnet (13). A second phase of this material undergoes a phase transition to a "canted antiferromagnetic" state at 36 K (14).

Bulky substituents have, on the other hand, not been employed before. We report here the synthesis and characterization of **6** in which a *tert*-butyl (^{t}Bu) group is located in the 5-position of the aromatic backbone. The effect of the bulky substituent on the structure is profound. Whereas **3** and **5** form stacked structures in which the molecules overlay directly, **6** has a stacked structure with every second layer reversed in order to accommodate the *tert*-butyl groups. It is the first example of a dithiadiazole that forms such *double-layer* stacks. Spacing within the stacks is much more regular than in

Scheme 1

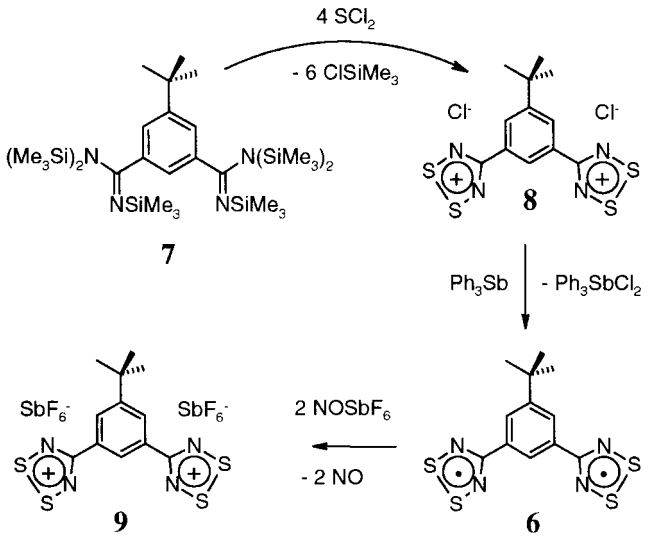

2, **3,** or **5**. The observed structure is consistent with a material that is stabilized *above* the Peierls distortion at room temperature, a conclusion substantiated by the magnetic susceptibility profile measured between 5 and 400 K.

In addition to a strong structural influence, the ^{t}Bu group has a solubilizing effect that has allowed measurements of the solution electrochemistry of **6**. Previously, **2** had been the only bifunctional dithiadiazole characterized by solution electrochemistry (15). The electrochemical behaviour of **6** supports previous conclusions that the two CN_2S_2 groups act as independent redox centres.

Results and discussion

Synthesis

Starting from the known 5-*tert*-butyl-1,3-dicyanobenzene (16), the persilylated amidine **7** was prepared using methods we have recently described in detail (17). Amidine **7** was fully characterized by chemical methods and by X-ray crystallography. In particular, it was important to be certain that both nitrile groups were derivatized to the amidine. Results of the structure determination are discussed below, while the spectroscopic properties are listed in the experimental section. Scheme 1 indicates the sequence of synthetic reactions used to prepare the title compound. **7** was condensed with sulfur dichloride (excess), and the resulting orange bisdithiadiazolium dichloride **8**, which was not further characterized, was reduced to the neutral diradical **6** using triphenylantimony. Purification of the crude diradical was performed by repetitive vacuum sublimation in a three-zone tube furnace at 10^{-2} Torr (1 Torr = 133.3 Pa), and crystals suitable for a diffraction study were grown in a furnace gradient of 50/100/180°C.

Oxidation of the diradical using nitrosyl hexafluoroantimonate afforded the SbF_6^- salt of the dication, **9**, which could be recrystallized as an orange solid containing solvent of crystallization. Compound **9** was used in the electrochemical studies described next.

Fig. 1. A typical steady-state cyclic voltammogram of **6** obtained in CH_2Cl_2 solution with 0.5 M NBu_4PF_6 electrolyte and containing the ferrocene internal voltammetric reference compound.

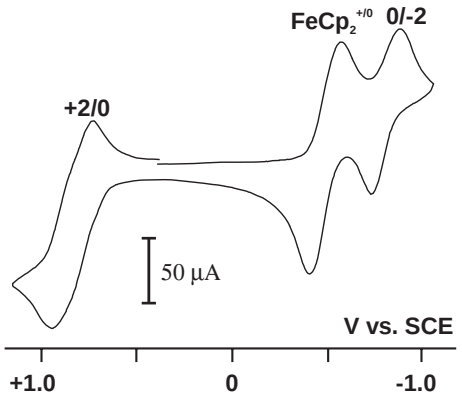

Table 1. Voltammetric data for the compounds.[a]

	$E_{1/2}$ / V			
	CH_3CN [b]		CH_2Cl_2 [c]	
Compound	Oxidation	Reduction	Oxidation	Reduction
6 (diradical)	Insoluble	Insoluble	+0.81	–0.79
9 (SbF_6^- salt)	+0.61 [d]	Not observed	Insoluble	Insoluble
2 (diradical) [e]	Insoluble	Insoluble	+0.78	–0.72
2 (SbF_6^- salt) [e]	+0.61 [f]	–0.80	Insoluble	Insoluble

[a] All potentials measured in *both* alternating current (a.c.) and cyclic voltammetry (cv) techniques.
[b] At a platinum electrode in CH_3CN containing 0.2 mol L^{-1} NBu_4PF_6 electrolyte, referenced to SCE such that $E_{1/2}$ = +0.38 for $[FeCp_2]^{+/-}$.
[c] At a platinum electrode in CH_2Cl_2 containing 0.5 mol L^{-1} NBu_4PF_6 electrolyte, referenced to SCE such that $E_{1/2}$ = +0.48 for $[FeCp_2]^{+/-}$.
[d] Separation between anodic and cathodic peak of 40 mV.
[e] Reference 15.
[f] Separation between anodic and cathodic peak of 30 mV.

Voltammetry and ESR spectroscopy

A combination of cyclic and a.c. voltammetry in typical organic solvents (CH_2Cl_2 and CH_3CN) was employed in an evacuated cell (18). We had previously investigated the electrochemical behaviour in solution of substituted aryl dithiadiazole radicals **1** as a function of substituent **X**, in a very rigorous procedure in which we obtained data in *both* solvents starting from either the free radical or a salt of a non-interacting anion (15, 19). We were also able to obtain acceptable cyclic voltammograms for the bifunctional diradical **2**, but only from CH_2Cl_2 solutions; similarly a salt of its dication could only be measured in CH_3CN. However, the isomeric **3** proved to be too insoluble for such studies. The ^{t}Bu group in **6** has a solubilizing effect, so that we were able to obtain reversible redox potentials for this compound in dichloromethane, and for the salt **9** in acetonitrile. For **6** in CH_2Cl_2 the oxidation process occurs at +0.81 V and the reduction at –0.79 V (vs. SCE). For the SbF_6^- salt, soluble only in CH_3CN, the 2-electron oxidation is observed at +0.61 V.

Voltammetric data for **6**, **9,** and **2** are compiled in Table 1. The redox potentials measured for the $2^+/2\cdot$ ("oxidation") and the $2\cdot/2^-$ ("reduction") processes are remarkably similar for the two forms **6** and **9** and the analogous versions (diradical and dication) of **2**. This confirms that the substituent effect of one dithiadiazole group attached to an aromatic ring on another similarly attached group is extremely small, and is independent of *meta* or *para* geometry. The two CN_2S_2 rings seem to behave independently. The 0.2 V difference between the potentials in acetonitrile and dichloromethane are typical for this ring system (15). The cell potentials, i.e., $\Delta E_{1/2}$, are also comparable to other dithiadiazole systems, and are larger than those observed for diselenadiazoles (15).

A typical steady-state cyclic voltammogram for the diradical measured in CH_2Cl_2 is presented in Fig. 1. There is a large separation between the anodic and cathodic peaks for both waves, with 250 mV for the oxidative and 190 mV for the reductive process. This is most likely due to the extremely low solubility of **6** in dichloromethane. (Thus a solution prepared by adding crystals of **6** to highly purified CH_2Cl_2 remains colourless, but has detectable ESR signals and voltammetric waves. However, the bulk solubility is negligible.) Similarly, with its concentration adjusted to that of the compound being studied, the reference compound, ferrocene, is almost equally broadened with a separation of 180 mV. The solubility of the cation from the salt **7** is considerably greater in acetonitrile, a solvent whose dielectric properties generally favour more "ideal" voltammograms. Only the oxidation process is reversible for this compound, a situation noted previously for monofunctional dithiadiazole cations. The absence of a reversible "reduction" wave, technically the second reduction starting from the dication, was attributed to a rapid comproportionation reaction between the small amount of anion formed and the large excess of cation (20).

There has been some discussion in the literature regarding the nature of the electron transfer processes in bifunctional dithiadiazoles (8, 21). Are the two groups on a single ring *simultaneously* oxidized or reduced? Can a radical cation or a radical anion be formed? These effects normally show up in the shapes of the cyclic voltammograms and size of the anodic–cathodic peak separations. We believe that a verdict has not been reached on this question. The data obtained for the "oxidation" process in acetonitrile (first reduction of the dication from **9**) are indicative of a two-electron step in which ΔE = 0, producing single peaks with a separation between anodic and cathodic peak of 40 mV, intermediate between those of a single (58 mV) and a two-electron (29 mV) process (22). However, the solubility of all bifunctional compounds prepared thus far is simply too low to draw authoritative conclusions.

ESR measurements show that there is a weak intramolecular exchange between the two radical centers on a single molecule at room temperature; intermolecular effects can be ruled out at the extremely low concentrations involved. Figure 2 shows limiting spectra in dichloromethane. At 250 K, a simple 5-line pattern due to hyperfine interaction to two equivalent ^{14}N nuclei is observed, with a_N = 0.51 mT. On warming, a more complex pattern develops, consistent with an intramolecular exchange coupling J_{ex} between radical centres that has probably not yet reached its limit at 340 K; at higher temperatures, the solvent boiled out of the resonant cavity. Exchange effects have been noted previously for diradicals, and the magnitude of the exchange process for **6** is intermediate between that of **2** and **3** (6, 7). The apparent absence of exchange phenomena in the electrochemistry may simply reflect

Fig. 2. X-Band ESR spectra of **6** at (*a*) 250 K and (*b*) 340 K measured in CH_2Cl_2 solution using 4 mm cylindrical quartz tubes.

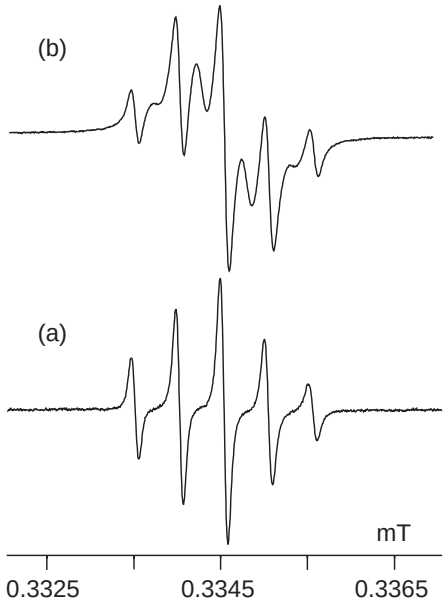

differences in the time scales of the cyclic voltammetry and ESR experiments.

In summary, the *tert*-butyl group is responsible for a marginal increase in solubility for the 1,3-bisdithiadiazole ring system, allowing the measurement of solution redox potentials for the first time. However, the solubility is still too low either for definitive electrochemical work on any cooperative effects between the two CN_2S_2 rings on a single molecule, or for detailed study of the intramolecular spin exchange mechanism by ESR. The preparation of more soluble derivatives is underway.

Table 2. Crystallographic data.

Compound	**6**	**7**
Formula	$C_{12}H_{12}N_4S_4$	$C_{30}H_{66}N_4Si_6$
fw	340.49	651.39
Crystal system	Tetragonal	Monoclinic
Space group	$I\bar{4}2m$ (No. 121)	$C2/c$ (No. 15)
a, Å	20.661(5)	10.078(3)
b, Å		21.328(5)
c, Å	6.764(7)	20.876(5)
β, deg		99.41(2)
V, Å^3	2887(1)	4426(1)
Z	8	4
ρ_{calc}, g cm^{-3}	1.566	0.977
F(000)	1408.00	1432.00
μ, cm^{-1}	6.51	2.10
Crystal size, mm	0.50 × 0.40 × 0.30	0.40 × 0.39 × 0.13
Temperature, K	250	200
Scan speed, deg min^{-1}	8.0 (in ω)	4.0 (in ω)
Scan range, deg	1.68 + 0.34 tan θ	1.47 + 0.34 tan θ
$2\theta_{max}$, deg	55.1	50.1
Crystal decay,%	0.99	0.11
Absorption correction	Empirical	Empirical
Absorption range	0.8510–1.0000	0.9624–1.0000
Total reflections	989	4276
Unique reflections	989	4026
R for merge		0.019
Data with $I \geq 3.00\sigma(I)$	499	1848
Solution method	Direct methods	Direct methods
Parameters refined	97	182
R	0.043	0.059
R_w	0.042	0.060
gof	2.07	2.0
Largest Δ/σ	0.52	0.001
Final difference map, e Å^{-3}	0.27	0.70

Rigaku AFC6S, MoK_α radiation (λ = 0.71069 Å); graphite monochromator, takeoff angle 6.0°, aperture 6 × 13 mm (horizontal × vertical) at a distance of 400 mm from the crystal, stationary background counts (scan/background time ratio 2:1), ω–2θ scans, empirical absorption correction applied based on azimuthal scans of several reflections, data corrected for Lorentz and polarization effects, solution by direct methods (SAPI91), refined by full-matrix least squares (DIRDIF94), function minimized $\sum w(|F_o| - |F_c|)^2$ where $w = 4F_o2/\sigma^2(F_o2)$, $R = \sum||F_o| - |F_c||/\sum|F_o|$, $R_w = (\sum w(|F_o| - |F_c|)^2/\sum|F_o|^2)^{1/2}$, and gof = $[\sum w(|F_o| - |F_c|)^2/(m - n)]^{1/2}$. Values given for R, R_w, and gof are based on those reflections with $I \geq 3.00\sigma(I)$.

Crystal and molecular structure of 7

A suitable single crystal of **7** was obtained by slow sublimation in a large round-bottomed sublimer, data crystals forming on the outside, air-cooled, region of the device. Data collection at low temperature helped to limit thermal motion of the many methyl groups in the molecule, and an *R*-factor of 6% was obtained with a data to parameter ratio of 10:1. Details of the structure determination and metric parameters are found in Tables 2–5. An ORTEP representation of the structure is presented in Fig. 3. The structure was refined in space group $C2/c$ with four molecules per unit cell. The molecule consistently occupies a special position, with C12, C14, and C15 all lying on a twofold rotation axis. This requires disorder in the positions of the three ^{t}Bu methyl groups. The disorder was modeled using two sets of methyl groups at half-occupancy with bond lengths constrained to 1.50 Å and isotropic temperature factors. The two amidine functional groups are crystallographically identical. The C10—N1 and C10—N2 distances are 1.410(5) and 1.264(5) Å, consistent with a C—N single and C═N double bond, respectively. For comparison, the distances in hexakis(trimethylsilyl)-1,4-benzdiamidine are 1.413(3) and 1.271(3) Å (23). All other molecular distances are unexceptional.

Crystal and molecular structure of 6

Several attempts to obtain data sets at lower temperatures did not lead to a satisfactory solution, but the data set collected at 250 K solved successfully. Details of the structure determination and metric parameters are found in Tables 2–5. An ORTEP representation of a single molecule is given in Fig. 4, which provides the atomic numbering scheme. In the molecular structure, the S—S, S—N, and N—C bond lengths agree closely with the experimental and calculated (square bracketed) values found for the $(HCN_2S_2)_2$ dimer: 2.07(3) [2.071]; 1.64(6) [1.635]; 1.32(8) [1.323] (24). They also compare closely with those found in **3**, which also crystallizes in a tetragonal space group, $I4_1/a$, and possesses a different layered structure, with pinwheel arrangement within the layers (6).

Much more interesting is the intermolecular structure. Two views of the crystal structure are presented in Figs. 5 and 6.

Table 3. Final atomic coordinates (fractional) and B_{eq}[a] (Å^2) for **6** and **7** ($\times 10^4$).

Atom	*x*	*y*	*z*	B_{iso}/B_{eq}
		6		
S(1)	0.70414(8)	0.02541(7)	0.255(1)	4.26(5)
S(2)	0.60713(8)	0.05153(8)	0.251(1)	4.95(5)
N(1)	0.7306(2)	0.0995(2)	0.263(3)	3.1(2)
N(2)	0.6213(2)	0.1294(2)	0.246(4)	4.0(1)
C(1)	0.6845(3)	0.1445(3)	0.247(4)	3.0(2)
C(2)	0.7043(3)	0.2140(3)	0.249(3)	2.4(1)
C(3)	0.7690(3)	0.2310	0.232(4)	2.1(1)
C(4)	0.6565(3)	0.2618(3)	0.233(3)	2.0(2)
C(5)	0.6734(3)	0.3266	0.252(5)	2.6(1)
C(6)	0.6204(3)	0.3796	0.226(5)	2.3(2)
C(7)	0.6422(5)	0.4411(5)	0.311(4)	13.7(7)
C(8)	0.6051(5)	0.3949	0.021(3)	8.5(4)
		7		
Si(1)	7516(2)	1383(1)	1656(1)	36(1)
Si(2)	5139(2)	2091(1)	793(1)	38(1)
Si(3)	2605(2)	414(1)	565(1)	38(1)
N(1)	5814(4)	1461(2)	1301(2)	29(1)
N(2)	4021(4)	860(2)	790(2)	32(1)
C(1)	8014(6)	555(3)	1816(3)	51(2)
C(2)	8606(6)	1683(3)	1076(3)	55(2)
C(3)	7892(6)	1826(3)	2429(3)	55(2)
C(4)	3424(6)	2284(3)	939(3)	51(2)
C(5)	6146(7)	2808(3)	1054(4)	71(2)
C(6)	5167(7)	1950(3)	–86(3)	58(2)
C(7)	1469(7)	882(4)	–55(4)	74(2)
C(8)	3067(7)	–316(3)	185(4)	69(2)
C(9)	1648(6)	230(3)	1233(3)	63(2)
C(10)	4895(5)	959(3)	1291(3)	28(1)
C(11)	4966(5)	610(1)	1922(2)	25(1)
C(12)	5000	932	2500	23(2)
C(13)	4938(6)	–41(2)	1929(3)	32(1)
C(14)	5000	–397(3)	2500	40(2)
C(15)	5000	–1075(3)	2500	73(3)
C(16)	5081	–1389	3148	56(4)
C(17)	3959	–1366	1991	58(4)
C(18)	6299	–1257	2288	133(7)

[a] $B_{eq} = 8/3\pi^2(U_{11}(aa^*)^2 + U_{22}(bb^*)^2 + U_{33}(cc^*)^2 + 2U_{12}aa^*bb^* \cos\gamma + 2U_{13}aa^*cc^* \cos\beta + 2U_{23}bb^*cc^* \cos\alpha)$

Table 4. Selected interatomic distances (Å) for **6** and **7**.

Atoms	Distance	Atoms	Distance
	6		
S(1)—S(2)	2.076(2)	S(1)—N(1)	1.627(4)
S(2)—N(2)	1.636(5)	N(1)—C(1)	1.335(7)
N(2)—C(1)	1.342(7)	C(1)—C(2)	1.494(7)
C(2)—C(3)	1.387(7)	C(2)—C(4)	1.402(8)
C(4)—C(5)	1.390(8)	C(5)—C(6)	1.56(1)
C(6)—C(7)	1.47(2)	C(6)—C(7)	1.47(2)
C(6)—C(8)	1.46(4)		
	7		
N(1)—Si(1)	1.762(4)	C(1)—Si(1)	1.853(6)
C(2)—Si(1)	1.874(6)	C(3)—Si(1)	1.856(6)
N(1)—Si(2)	1.776(4)	C(4)—Si(2)	1.851(6)
C(5)—Si(2)	1.867(6)	C(6)—Si(2)	1.863(6)
C(8)—Si(3)	1.841(7)	C(9)—Si(3)	1.862(7)
C(10)—N(1)	1.414(6)	C(10)—N(2)	1.270(6)
C(11)—C(10)	1.503(7)	C(12)—C(11)	1.384(2)
C(15)—C(14)	1.446(7)		

Table 5. Selected bond angles (°) for **6** and **7**.

Atoms	Angle	Atoms	Angle
	6		
S(2)S(1)-N(1)	94.6(2)	S(1)-S(2)-N(2)	94.8(2)
S(1)-N(1)-C(1)	114.3(4)	S(2)-N(2)-C(1)	113.7(4)
N(1)-C(1)-N(2)	122.2(5)	N(1)-C(1)-C(2)	118.2(5)
N(2)-C(1)-C(2)	119.3(5)	C(1)-C(2)-C(3)	120.5(6)
C(1)-C(2)-C(4)	118.9(5)	C(3)-C(2)-C(4)	119.6(7)
C(2)-C(3)-C(2)	118.8(8)	C(2)-C(4)-C(5)	119.6(6)
C(4)-C(5)-C(4)	118.5(g)	C(4)-C(5)-C(6)	119.3(7)
C(4)-C(5)-C(6)	119.3(7)	C(5)-C(6)-C(7)	110(1)
C(5)-C(6)-C(7)	110(1)	C(5)-C(6)-C(8)	114(2)
C(7)-C(6)-C(7)	112(2)	C(7)-C(6)-C(8)	104(1)
C(7)-C(6)-C(8)	104(1)		
	7		
Si(2)-N(1)-Si(1)	125.0(3)	C(10)-N(1)-Si(1)	121.6(4)
C(10)-N(1)-Si(2)	112.2(3)	C(10)-N(2)-Si(3)	138.7(4)
N(2)-C(10)-N(1)	120.1(5)	C(11)-C(10)-N(1)	115.2(4)
C(11)-C(10)-N(2)	124.5(5)	C(12)-C(11)-C(10)	120.6(3)
C(11)-C(12)-C(11)	120.6(4)	C(14)-C(13)-C(11)	123.5(5)
C(13)-C(14)-C(13)	114.5(6)	C(15)-C(14)-C(13)	122.8(3)

There are eight molecules per unit cell. At the center of the cell is located a $\bar{4}$ symmetry axis, perpendicular to the plane shown in Fig. 5, and passing through the point {1/2,1/2,0}. This axis defines the packing of the ^{t}Bu groups: diagonally opposed groups are at the same level; neighbouring groups are half a *c* translation apart, resulting in a double helical staircase of ^{t}Bu groups surrounding an infinite channel lined by hydrogen atoms. A more complex channel is located at the other $\bar{4}$ axis perpendicular to *c*, which passes through the family of points {1/2,0,0}. To depict this channel more accurately, four additional molecules have been added to the unit cell in the *–b* direction in Fig. 5.[3] In all, eight CN_2S_2 rings contribute to the two layers of the depicted channel. Consistent with the $\bar{4}$ symmetry, the pinwheel geometry of four CN_2S_2 rings is *reversed* every second layer, so that the infinite channel lined by sulfur atoms is defined by two *contrarotating* pinwheel groups of dithiadiazole rings. Whereas the pinwheel motif has been seen in numerous dithiadiazole structures, this is the first example of contrarotating double layers of pinwheels.

Each molecule of **6** is centred on a 2_1 screw axis parallel to *c* and passing through the point {1/4,1/4,0}, defining a forward–backward packing motif for each subsequent molecule of **6** in an infinite stack. That this motif is adopted in order to accommodate the bulky ^{t}Bu groups while maintaining as many intermolecular S···S and S···N contacts as possible seems almost certain, since both **3** and **5** have structures in which the

[3] The channel is quite narrow, having a diameter of only 1.3 Å when the van der Waals' radius of sulfur is taken as 1.80 Å.

Fig. 3. ORTEP representation, showing the atom numbering scheme, of a single molecule of **7** as it is found in the crystal structure. The molecule lies on a twofold rotation axis, and the *t*Bu group is disordered. In the refinement two constrained groups (half-occupancy) with isotropic temperature factors were allowed; only a single group has been drawn in the picture.

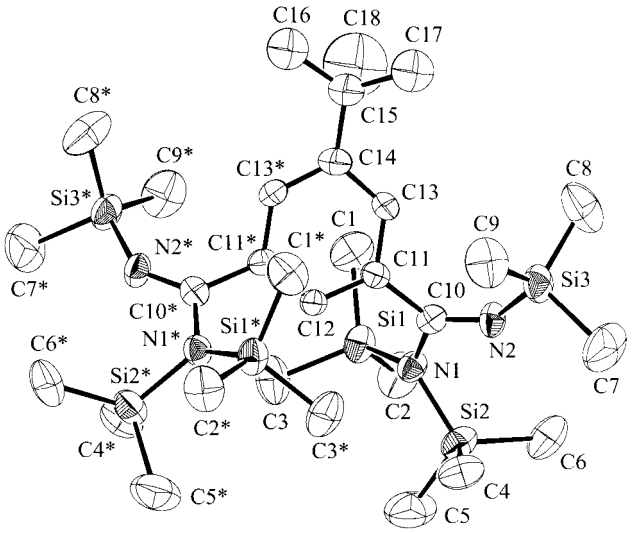

Fig. 4. ORTEP representation, showing the atom numbering scheme, of a single molecule of **6** as it is found in the crystal structure.

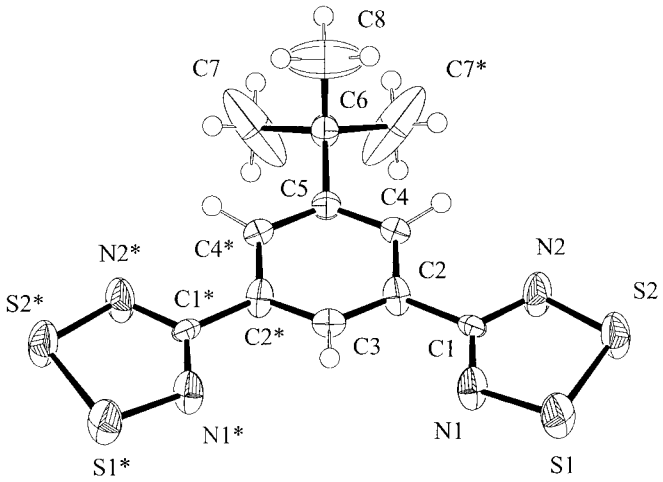

bent 1,3-$(S_2N_2C)C_6H_3$ units lie directly above one another in a superimposed infinite stack. Spacing between the layers in **6** is much more even than in either **3** or **5**. This is shown very clearly in Fig. 6, which is a view perpendicular to the *a* axis depicting only the CN_2S_2 units of a single sulfur channel. The unit cell diagonals are mirror planes; consistently, the two halves of each molecule of **6** are identical by symmetry and the *t*Bu groups are ordered. The crystal symmetry does not require planarity of the molecules. Consistently, the CN_2S_2 rings are both canted and cupped slightly at the equilibrium distance of the structure determined at 250 K. However, the thermal ellipsoids (Fig. 4) are elongated in the perpendicular direction, so that we expect there to be considerable rocking vibration. At the equilibrium distances determined in the structure, each layer is separated by two slightly longer and two slightly shorter interstack S···S distances, at 3.48(2) and 3.61(2) Å. These distances should be compared to the mean short and long distances in **3** (3.140 and 3.966 Å) and in **5** (3.12 and 3.89 Å). The mean distances are much more comparable: 3.55 in **3** and **6**, 3.51 in **5**. However, since the S···S contacts in **6** are at an angle to the perpendicular, it follows that the ring centroid-to-centroid distance in **6** at 3.382 Å is considerably

Fig. 5. PLUTO representation of the crystal packing observed in the solid-state structure of **6**. The view is down the *c* axis, and the range of indices plotted is *a*: 0–1; *b*: –1/2–1; *c*: 0–1. Heavy solid and broken lines represent the intermolecular sulfur–sulfur contacts at S2 on the upper (black) and lower (gray) layers, as well as between layers at S1.

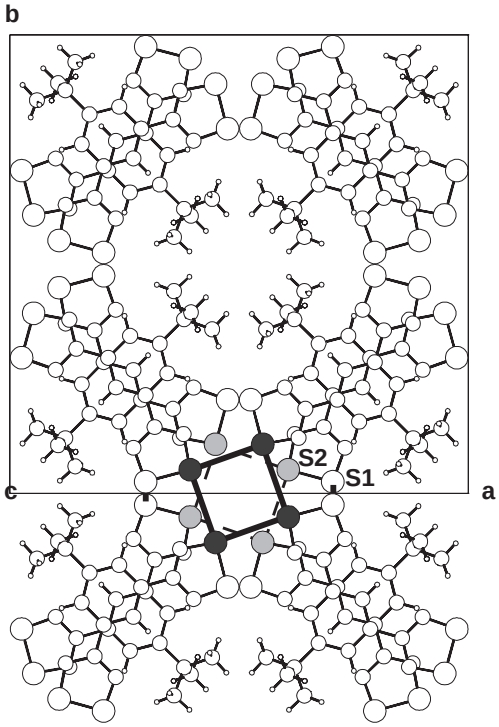

Fig. 6. Side view of portion of a single infinite sulfur-lined channel centred on a $\bar{4}$ axis. Only the CN_2S_2 rings are drawn in this PLUTO representation. The larger diameter spheres are the sulfur atoms.

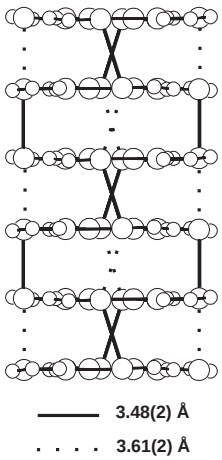

shorter than that in **3** (3.631) and **5** (3.52 Å). Indeed in **6** the separation approaches that in graphite (3.35 Å) (25). The offset packing of the benzene rings in **6** is highly reminiscent of the ground-state structure of graphite, while in **3** and **5** the C_6 rings are directly superimposed.

The pinwheels in each layer are identical except for the direction of rotation. The cross-ring contacts are all 3.474(2) Å between the S2 atoms on adjacent rings. These contacts are noticeably *longer* than in **3** (3.140 and 3.284 Å), which has a pinwheel structure (6), but shorter than the interactions in the lower-symmetry structure of **5** (9). It may be that despite the central $\bar{4}$ symmetry, the ^{t}Bu groups generate considerable steric hindrance and that this prevents the S1 atoms from lining up into a truly vertical column. The calculated density of the structure is consistently the lowest of any bifunctional neutral dithiadiazole (1.57 g cm^{-3}, vs. a range of 1.61– 2.26 for a variety of bifunctional species (6–8)).

In summary, the crystal structure of **6** is a unique double-layered stacking type. This structure is adopted to accommodate the bulk of the ^{t}Bu groups while still maintaining interlayer contacts among the sulfur atoms. Contrary to previous belief, bulky substituents can be useful molecular engineering tools for the development of stacking dithiadiazole radicals. There are no secondary S–X interactions since there are no other donor sites in the molecules. However, steric repulsion among the bulky substituents may be hindering an even more efficient packing, as reflected in the long cross-stack distances. It may be that modification of the substituents while maintaining bulk (^{i}Pr, CF_3, CCl_3), with or without symmetry lowering, may lead to other double-layer stacked structures with tighter packing within the stacks.

Magnetism and conductivity

The magnetic susceptibility of the title compound was measured as a function of temperature and the results are presented in Fig. 7.[4] The response of the sample to magnetization is complex, typical of bifunctional dithiadiazole systems (4, 6, 7). At very low temperature the sample obeys the Curie–Weiss Law, with $\theta = 0$ K and $\chi_0 = -156$ ppm emu mol^{-1}. The free-spin concentration at absolute zero is estimated to be 1.3%, reflecting paramagnetic defects in an essentially diamagnetic structure. The diamagnetism starts to lift above 210 K, and there is a distinct kink in the susceptibility v*s. T* response at 260 K. A plot of χT vs. *T* (Fig. 7*b*) is linear for the points recorded above 260 K, indicative of an antiferromagnetic exchange interaction in this temperature range. At room temperature, the magnetization corresponds to approximately 0.30 unpaired electrons *per molecule*. The susceptibility data bear remarkable similarity to those of **3** and **5**, *except that the onset of paramagnetism is found 200 K lower in the title compound*. The room temperature pressed-pellet conductivity of the material is less than 10^{-7} S cm^{-1}; this absence of conductivity, given a rich source of carriers, is often observed for neutral dithiadiazoles, leading to the conclusion that their bandwidths are narrow (4). In effect they are Mott insulators (26). The observed structure, consistent with the magnetic behaviour, suggests that the orientation imposed on the title compound by the bulky ^{t}Bu group has stabilized it *above* the Peierls distortion at room temperature, the first stacking neutral dithiadiazole for which this has been achieved. The crystal symmetry of the 250 K structure allows a range of structures from alternating long–short–long S1···S1 distances to completely even spacing. It is possible that below 210 K a greater distortion sets in to produce a fully diamagnetic structure, and in support of this hypothesis several X-ray data sets collected between 150 and 250 K did not lead to satisfactory solutions.

In summary, the novel "double-layer" geometry adopted by the title compound is a consequence of having to pack the large ^{t}Bu group efficiently while preserving intermolecular S···S and S···N contacts. This leads to the unusual dithiadiazole stacking pattern in which a *single* sulfur atom chain maintains contacts down the stack, but with weak interstack interactions. The most dramatic effect of the structure adopted by **6** is on the magnetic behaviour, with the onset of paramagnetism 200 K lower in temperature than in **3** or **5**. Recently some distorted bifunctional dithiadiazoles with biphenyl spacers have shown a slight lowering of the onset temperature (ca. 50 K),[5] but nothing as dramatic as in **6**. Optimization of the spacing substituent may finally allow the preparation of densely stacked neutral dithiadiazoles with equal spacing at room temperature and a sufficiently high bandwidth to achieve a conducting state. Alternatively, bulky groups may find great utility in designing molecular magnets from isolated dithiadiazole groups, a goal recently advanced by others (14). Efforts in both of these directions are underway.

Experimental section

Starting materials and general procedures

5-*tert*-Butylisophthalic acid, sulfur dichloride, 1,1,1,3,3,3-hexamethyldisilazane, *n*-butyllithium, thionyl chloride, ammonium hydroxide, chlorotrimethylsilane, nitrosonium hexafluoroantimonate, and triphenylantimony were all obtained commercially (Aldrich). Sulfur dichloride was distilled before use. Lithium bis(trimethylsilyl)amide diethyl etherate was prepared as described previously (17). Acetonitrile (Fisher HPLC grade) was distilled from phosphorus pentoxide, and toluene from sodium metal. All reactions were performed under an atmosphere of dry nitrogen. NMR spectra were acquired at 250.13 (^{1}H) and 62.90 (^{13}C) MHz on a Bruker AC250-F spectrometer, and ESR spectra on a Bruker EMX instrument. Infrared spectra were obtained as Nujol mulls or KBr pellets on a Bomen MB102 instrument. Elemental analyses were performed by MHW Laboratories, Phoenix, Ariz., and mass spectra were recorded by the Mass Spectrometry Center, University of Alberta, Edmonton.

Preparation of 5-*tert*-butyl-1,3-[$(Me_3Si)_2NCNSiMe_3]_2C_6H_3$, (5-^{t}Bu-1,3-DIBADS)

Solid 5-*tert*-butylisophthalonitrile (46.06 g, 250 mmol) (16) was added to a slurry of lithium bis(trimethylsilyl)amide diethyl etherate (120.75 g, 500 mmol) in 1500 mL of toluene and the mixture was then stirred overnight at 50–70°C. Chlorotrimethylsilane (96 mL, 750 mmol) was added and the mixture

[4] The measurement was performed by R.C. Haddon and T.T.M. Palstra at Bell Laboratories (Lucent Technologies, Murray Hill, N.J.) using a SQUID magnetometer operating at 1 tesla.

[5] T.M. Barclay, A.W. Cordes, N.A. George, R.T. Oakley, and R.C. Haddon, 80th Canadian Society for Chemistry Conference, Windsor, Ontario, July 1–4, 1997. Abstract No. 335.

heated to a gentle reflux for an additional 48 h. The mixture was then cooled and filtered (LiCl) and the solvent removed in vacuo. The residual oil was dissolved in 30 mL of hot toluene and 20 mL of acetonitrile was added while the solution was still hot. After cooling to room temperature an additional 20 mL acetonitrile was added to the solution after which it was cooled to –30°C overnight to give crystalline 5-^{t}Bu-1,3-DIBADS (56.89 g, 0.0873 mol, 35%), mp 118–120°C. IR (KBr pellet): 2972 (vs), 2905 (sh), 1638 (br), 1481 (m), 1362 (m), 1310 (m), 1252 (vs), 1215 (vs), 1148 (s), 1119 (m), 1036 (m), 1011 (m), 907 (vs), 841 (br), 747 (s), 724 (s), 694 (s), 658 (m), 629 (m), 585 (w), 555 (w), 497 (w), 424 (m), 379 (w), 345 (m). ^{1}H NMR (δ, $CDCl_3$): 0.066 (s, 54 H, $SiMe_3$), 1.32 (s, 9 H, ^{t}Bu), 7.17 (t, 1.55 Hz, 1 H, phenylene), 7.33 (d, 1.55 Hz, 2 H, phenylene). ^{13}C NMR: 2.66, 31.2, 34.8, 124.9, 126.9, 142.6, 149.7, 167.0. Mass spectrum, *m/z:* 651 ($C_4H_9C_6H_3[CN_2Si(CH_3)_3]_2^+$, 42%), 635 ($C_3H_6C_6H_3[CN_2(Si(CH_3)_3]_2^+$, 12%), 547 ($C_4H_8C_6H_3CN_2$-$(Si(CH_3)_3)_3CN_2(Si(CH_3)_3)_2^+$, 13%), 506 ($C_4H_7C_6H_3[CN_2$-$(Si(CH_3)_3]_2^+$, 6%), 490 ($C_3H_3C_6H_3[CN_2(Si(CH_3)_3)_2]_2^+$, 12%), 390 ($C_4H_7C_6H_3CN_2(Si(CH_3)_3)_3^+$, 13%), 259 ($CN_2(Si(CH_3)_3)_2^+$, 14%), 73 ($Si(CH_3)_3^+$, 100%). Anal. calcd. for $C_{30}H_{66}N_4Si_6$: C 55.32, H 10.21, N 8.60%; found: C 55.32, H 9.96, N 8.60%.

Preparation of 5-*tert*-butyl-1,3-$(S_2N_2C)_2C_6H_3$

Sulfur dichloride (7.5 mL, 120 mmol) was added, while stirring, to a slurry of 5-^{t}Bu-1,3-DIBADS (6.1 g, 9.36 mmol) in 150 mL of acetonitrile. The resulting mixture was heated to a gentle reflux for 3 h and then filtered to afford crude 5-^{t}Bu-1,3-$[(S_2N_2C)_2C_6H_3]^{2+}(Cl^-)_2$ (2.56 g, 6.22 mmol, 80%) as an orange solid that was dried in vacuo overnight. Ph_3Sb (2.42 g, 6.84 mmol) was added to a stirring slurry of the orange solid in 65 mL of degassed CH_3CN and the mixture was refluxed for 2 h. The crude product (2.01g, 5.9 mmol, 95%), which is both oxygen and moisture sensitive, was then slowly sublimed in a three-zone (50/100/170–180°C) tube furnace over 4 days at 1×10^{-2} Torr to produce large black crystals, collected in the 170°C range (0.589 g, 1.73 mmol, 28%), that are much less air sensitive than the crude product. This was resublimed to produce analytical samples of product, mp 258–262°C. IR (1700–250 cm^{-1}): 1678 (w), 1603 (w), 1551 (w), 1339 (vs), 1273 (m), 1217 (w), 1103 (br), 993 (m), 951 (w), 910 (w), 891 (w), 837 (w), 799 (vs), 706 (w), 691 (vs), 679 (sh), 577 (w), 511 (m). Mass spectrum, *m/z:* 340 ($C_4H_9C_6H_6(CN_2S_2)_2^+$, 100%), 325 ($C_3H_6C_6H_3(CN_2S_2)_2^+$, 18%), 294 ($C_4H_9C_6H_3$-$CN_2S_2CNS^+$, 16%), 262 ($C_4H_9C_6H_3CN_2S_2CN^+$, 67%), 247 ($C_3H_6C_6H_3CN_2S_2CN^+$, 14%), 169 ($C_3H_6C_6H_3(CN)_2^+$, 23%), 141 ($C_3H_6C_6H_3C_2^+$, 31%), 78 ($S_2N^+$, 55%). Anal. calcd. for $C_{12}H_{12}N_4S_4$: C 42.33, H 3.55, N 16.45%; found: C 42.44, H 3.40, N 16.51%.

Preparation of 5-*tert*-butyl-1,3$[(S_2N_2C)_2C_6H_3]^{2+}$ $(SbF_6^-)_2$

5-^{t}Bu-1,3$[C_6H_3(CN_2S_2)_2]^{2+}$ $(Cl^-)_2$ (1.0 g, 2.43 mmol) and nitrosonium hexafluoroantimonate (1.29 g, 4.86 mmol) were added to a 250 mL side-arm flask followed by 5 mL acetonitrile. After gentle reflux for 1 h, the solvent was evaporated in a stream of N_2 (g). The crude product was dissolved in 60 mL of dichloromethane and a minimum amount of acetonitrile (15–20 mL). After cooling to –30°C, crystalline **9** was collected by cold filtration. Yield 0.71 g, 0.874 mmol, 36%, mp (dec.) 205–211°C. IR (1700–250 cm^{-1}): 1689 (w), 1603 (w), 1418 (m), 1356 (vs), 1271 (m), 1211 (w), 1123 (br), 1038 (w), 1017 (w), 968 (w), 899 (m), 837 (sh), 720 (m), 662 (vs), 552 (w), 289 (s). Anal. calcd. for $C_{12}H_{12}N_4S_4Sb_2F_{12}$: C 17.75, H 1.49, N 6.90%; found: C 17.65, H 1.44, N 6.78%. The solid was insufficiently volatile to yield a mass spectrum.

Fig. 7. Plots of (*a*) the magnetic susceptibility of **6** as a function of temperature, and (*b*) the fraction of Curie spins per molecule, determined from the susceptibility data, as a function of temperature.

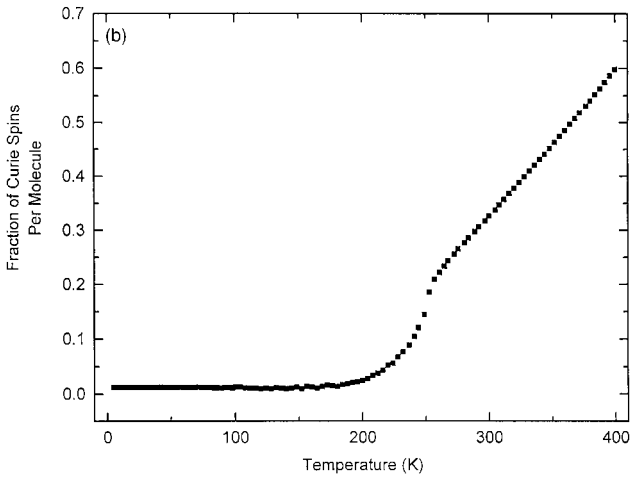

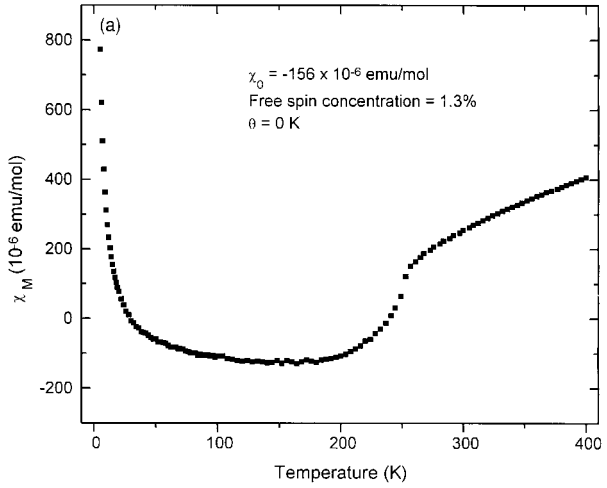

Crystal structure determination.

Crystallographic data appear in Table 2. The final unit-cell parameters were obtained by least squares on the setting angles for 25 reflections with 2θ = 20.2°–30.0° for **7** and for 14 reflections with 2θ = 18.5°–21.5° for **6**. Hydrogen atoms were included at geometrically idealized positions (C—H 0.95 Å), but were not refined. All non-hydrogen atoms were refined anisotropically. Scattering factors were those of Cromer and Waber (27), and allowance was made for anomalous dispersion (28). Computer programs used at Calgary include SAPI91 (29), DIRDIF94 (30), and teXsan (31); and, at Lethbridge, NRC386, a PC version of NRCVAX (31). Final fractional coordinates and B_{eq} appear in Table 3, selected interatomic distances in Table 4, and selected bond angles in Table 5. ORTEP diagrams showing the atomic numbering scheme are presented in

Fig. 3 (**7**) and Fig. 4 (**6**). Crystal structure reports, and additional tables of final positional parameters, bond lengths and angles, hydrogen atom coordinates, and anisotropic displacement parameters for both **6** and **7** have been deposited as supplementary material.[6]

Electrochemistry

For the voltammetric experiments the vacuum-tight all-glass cell with Pt electrodes that has been described previously (18) was employed. The cell was charged with electrolyte ($N^nBu_4PF_6$) and the solvent, dry degassed CH_3CN or CH_2Cl_2, was transferred on a vacuum line. Samples and ferrocene as an internal reference were added to the cell using break-seal techniques. The ferricenium/ferrocene couple is observed in this system at +0.38 V (CH_3CN) and +0.48 V (CH_2Cl_2) vs. SCE at 25°C. Cyclic voltammetric (scan rates $\nu = 20–500$ mV s^{-1}) and phase-sensitive alternating current experiments ($\omega = 610$ Hz, $\nu = 10$ mV s^{-1}) were carried out with a PAR 170 electrochemical system.

Acknowledgments

We thank Prof. Robert Thompson, University of British Columbia, for a preliminary magnetic susceptibility measurement at room temperature, and Dr. Robert Haddon, Bell Labs, for the VT measurements. Dr. Ralph Weber of Bruker, U.S.A., provided time on the EMX spectrometer, and we thank the staff at Bruker for their assistance. The Natural Sciences and Engineering Research Council of Canada and the University of Lethbridge Research Fund provided financial support.

References

1. (*a*) R.T. Oakley. Can. J. Chem. **71**, 1775 (1993); (*b*) A.W. Cordes, R.C. Haddon, and R.T. Oakley. *In* The chemistry of inorganic ring systems. *Edited by* R. Steudel. Elsevier, Amsterdam. 1992. p. 295; (*c*) A.J. Banister and J.M. Rawson. *In* The chemistry of inorganic ring systems. *Edited by* R. Steudel. Elsevier, Amsterdam. 1992. p. 323; (*d*) J.M. Rawson, A.J. Banister, and I. Lavender. Adv. Heterocycl. Chem. **62**, 137 (1995).
2. A. Vegas, A. Pérez-Salazar, A.J. Banister, and R.G. Hey. J. Chem. Soc. Dalton Trans. 1812 (1980).
3. A.W. Cordes, R.C. Haddon, and R.T. Oakley. Adv. Mater. **6**, 798 (1994).
4. C.D. Bryan, A.W. Cordes, R.M. Fleming, N.A. George, S.H. Glarum, R.C. Haddon, C.D. MacKinnon, R.T. Oakley, T.T.M. Palstra, and A.S. Perel. J. Am. Chem. Soc. **117**, 6880 (1995).
5. C.D. Bryan, A.W. Cordes, R.C. Haddon, R.G. Hicks, D.K. Kennepohl, C.D. MacKinnon, R.T. Oakley, T.T.M. Palstra, A.S. Perel, S.R. Scott, L.F. Schneemeyer, and J.V. Waszczak. J. Am. Chem. Soc. **116**, 1205 (1994).
6. M.P. Andrews, A.W. Cordes, D.C. Douglass, R.M. Fleming, S.H. Glarum, R.C. Haddon, P. Marsh, R.T. Oakley, T.T.M. Palstra, L.F. Schneemeyer, G.W. Trucks, R. Tycko, J.V. Waszczak, K.M. Young, and N.M. Zimmerman. J. Am. Chem. Soc. **113**, 3559 (1991).
7. A.W. Cordes, R.C. Haddon, R.T. Oakley, L.F. Schneemeyer, J.V. Waszczak, K.M. Young, and N.M. Zimmerman. J. Am. Chem. Soc. **113**, 582 (1991).
8. C.D. Bryan, A.W. Cordes, J.D. Goddard, R.C Haddon, R.G. Hicks, C.D. MacKinnon, R.C. Mawhinney, R.T. Oakley, T.T.M. Palstra, and A.S. Perel. J. Am. Chem. Soc. **118**, 330 (1996).
9. A.W. Cordes, R.C. Haddon, R.G. Hicks, D.K. Kennepohl, R.T. Oakley, T.T.M. Palstra, L.F. Schneemeyer, S.R. Scott, and J.V. Waszczak. Chem. Mater. **5**, 820 (1993).
10. W.M. Davis, R.G. Hicks, R.T. Oakley, B. Zhao, and N.J. Taylor. Can. J. Chem. **71**, 180 (1993).
11. A.W. Cordes, R.C. Haddon, R.G. Hicks, R.T. Oakley, and T.T.M. Palstra. Inorg. Chem. **31**, 1802 (1992).
12. A.W. Cordes, R.C. Haddon, R.G. Hicks, D.K. Kennepohl, R.T. Oakley, L.F. Schneemeyer, and J.V. Waszczak. Inorg. Chem. **32**, 1554 (1993).
13. A.J. Banister, N. Bricklebank, W. Clegg, M.R.J. Elsegood, C.I. Gregory, I. Lavender, J.M. Rawson, and B.K. Tanner. J. Chem. Soc. Chem. Commun. 679 (1995).
14. A.J. Banister, N. Bricklebank, I. Lavender, J.M. Rawson, C.I. Gregory, B.K. Tanner, W. Clegg, M.R.J. Elsegood, and F. Palacio. Angew. Chem. Int. Ed. Engl. **35**, 2533 (1996).
15. R.T. Boeré and K.H. Moock. J. Am. Chem. Soc. **117**, 4775 (1995).
16. M.A. McCall, J.R. Caldwell, H.G. Moore, and H.M. Beard. J. Macromol. Sci. Chem. **A3**, 911 (1969).
17. R.T. Boeré, R.G. Hicks, and R.T. Oakley. Inorg. Synth. **21**, 94 (1997).
18. K.H. Moock and M.H. Rock. J. Chem. Soc. Dalton Trans. 2459 (1993).
19. R.T. Boeré, K.H. Moock, and M.Z. Parvez. Z. Anorg. Allg. Chem. **520**, 1589 (1994).
20. C.M. Aherne, A.J. Banister, I.B. Gorrell, M.I. Hansford, Z.V. Hauptman, A.W. Luke, and J.M. Rawson. J. Chem. Soc. Dalton Trans. 967 (1993).
21. P. Del Bel Belluz, A.W. Cordes, E.M. Kristof, P.V. Kristof, S.W. Liblong, and R.T. Oakley. J. Am. Chem. Soc. **111**, 9276 (1989).
22. J.B. Flanagan, S. Margel, A.J. Bard, and F.C. Anson. J. Am. Chem. Soc. **100**, 4248 (1978).
23. F. Weller, F. Schmock, and K. Dehnicke. Z. Naturforsch. B: Chem. Sci. **44**, 548 (1989).
24. A.W. Cordes, C.D. Bryan, W.M. Davis, R.H. de Laat, S.H. Glarum, J.D. Goddard, R.C. Haddon, R.G. Hicks, D.K. Kennepohl, R.T.Oakley, S.R. Scott, and N.P.C. Westwood. J. Am. Chem. Soc. **115**, 7232 (1993).
25. F.A. Cotton and G. Wilkinson. Advanced inorganic chemistry. 3rd ed. Wiley, New York. 1972. p. 288.
26. P.A. Cox. Electronic structure and chemistry of solids. Oxford University Press, Oxford. 1987. p. 134.
27. D.T. Cromer and J.T. Waber. International tables for X-ray crystallography. Vol. IV. The Kynoch Press, Birmingham, England. 1974. Table 2.2 A.
28. D.C. Creagh and W.J. McAuley. International tables for crystallography. Vol C. *Edited by* A.J.C. Wilson. Kluwer Academic Publishers, Boston. 1992. Table 4.2.6.8, pp. 219–222.
29. H.-F. Fan. Structure analysis programs with intelligent control. Rigaku Corporation, Tokyo. 1991.
30. P.T. Beurskens, G. Admiraal, G. Beurskens, W.P. Bosman, R. de Gelder, R. Israel, and J.M.M. Smits. The DIRDIF-94 program system. Technical Report of the Crystallography Laboratory, University of Nijmegen, The Netherlands. 1992.
31. TEXSAN. Single-crystal structure analysis software. Molecular Structure Corporation, The Woodlands, Texas. 1994.
32. E.J. Gabe, Y. LePage, J.P. Charland, F.L. Lee, and P.S. White. J. Appl. Crystallogr. **22**, 348 (1989).

[6] This material may be purchased from: The Depository of Unpublished Data, Document Delivery, CISTI, National Research Council Canada, Ottawa, Canada K1A 0S2. The crystal structure reports, including tables of bond lengths, bond angles, and atomic coordinates, have also been deposited with the Cambridge Crystallographic Data Centre, and can be obtained on request from The Director, Cambridge Crystallographic Data Centre, University Chemical Laboratory, 12 Union Road, Cambridge, CB2 1EZ, U.K.